Measuring RF currents induced in implants using B1+ maps

Mélina Bouldi[1] and Jan M. Warnking[1,2]
[1]*Grenoble Institut des Neurosciences - UJF, Grenoble, Rhônes Alpes, France*, [2]*Inserm U836, Grenoble, Rhônes Alpes, France*

Target audiences : MR physicists and engineers

Purpose:

Assessing MR RF safety in the presence of conducting implants may require measurement of induced SAR in individual subjects, due to a potentially large variability of implant geometry and position. MR thermometry suffers from susceptibility artifacts close to the implant as well as limited sensitivity. B_1^+ field distortions generated by induced RF currents may allow quantitative measurement of those currents radipdly and with a low SAR, and thus prediction of induced SAR. We improve on a published method developed in [1], using electromagnetic simulation in addition to experimental studies on ASTM phantom, to validate the theoretical model.

Theory:

In the presence of a conductive wire, the measured RF field B_1^{total} is the complex sum of 2 components: the first one generated by the transmit coil, B_1^{magnet}, and the other by the induced current in the long conductive wire, B_1^{wire}. Using Ampere's law and the expression of the field calculated by [2], we obtained the expression of the induced component (Eq.1). It depends on: the position of the voxel, expressed in cylindrical coordinates (r, θ, z) with respect to the wire axis, the induced current I, the current's phase relative to the magnet field θ_0 and the azimuthal angle θ. B_1^{magnet} was assumed to be constant over a region close to the wire implant.

$$B_1^{wire}(r,\theta,z) = \frac{\mu_0 \mu_r I(z)}{4\pi|\vec{r}|} e^{-i(\theta-\theta_0)} \quad \textbf{Eq.1}$$

Materials and methods:

Experimental set-up: A phantom, built according to ASTM F2182-09 [3], was filled with a medium consisting of sodium chloride (1 g/L) and hydroxyethyl-cellulose (25 g/L) in water, with a low frequency conductivity of 0.55 S/m (Conductimeter Mettler Toledo®). A 20 cm long copper wire of 3 mm diameter, insulated with a thin film of varnish along its length and bare at the tips, was placed at 5.5 cm of the left border of the container, aligned with the static field direction. The phantom was centered in a 3-T TX Achieva MR scanner (Philips Healthcare®). The system body coil was used for RF transmission. The transmitted radiofrequency field B_1 was obtained by an actual flip angle imaging (AFI) pulse sequence [4], with TR_1 = 30 ms and TR_2 = 150 ms.

Electromagnetic simulations: Simulations were performed using commercial FDTD software (SEMCAD®, version 14.8, SPEAG, Zürich). We aimed to implement a numerical model of the whole body RF transmit resonator resembling the present resonator as closely as possible. The actual resonator in our system is slightly elliptical, so the structure chosen for the RF coil was an elliptical 16-leg birdcage coil, with an aspect ratio of 3:2.75, shielded, band-pass [5]. The excitation was sinusoidal (16 sources, situated in the middle of each leg, with successive current phases shifted by $2\pi/16$). We adjusted the capacities in legs and end-rings to tune the birdcage to 128 MHz. The birdcage was loaded with a thermally insulated phantom model and a wire model close to real ones.

Data processing: Experimental data B_1^{mes} were fitted to the absolute $B_1^{total} = |B_1^{magnet} + B_1^{wire}|$ obtained from the theoretical model. The fit was performed simultaneously over all voxels inside a ROI of 27x27x210 mm surrounding the wire, excluding the voxels closest to the wire where experimental B_1 data were limited in dynamic range. Fit parameters included the magnitude of the wire current at each z-position, the current phase (common to all z-positions) and the static B_1^{magnet}. The current profile along the wire obtained from the fit was subsequently compared to the results of the EM simulation.

Results and discussion:

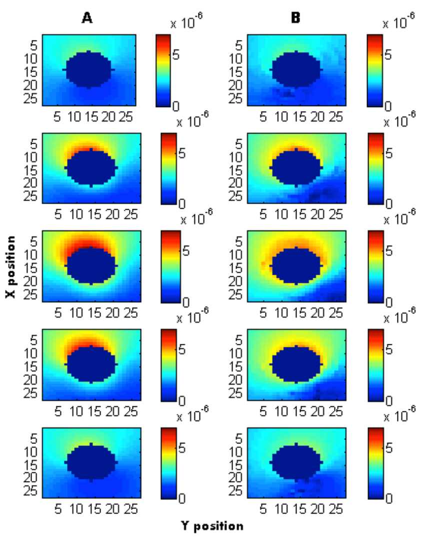

Fig. 1

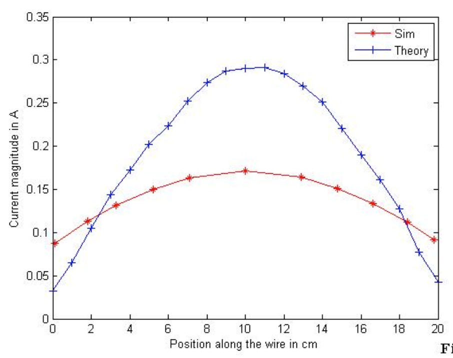

Fig. 2

Fig.1: A*) Theoretical* B_1^{total} *along the wire, at 5 distinct z-values.* B*) Experimental* B_1^{total} *at the same position.*

Fig.2: *Simulated current (in red/star) and fitted current (in blue/cross), along the wire.*

B_1 maps along the wire (Fig.1) present good concordance between theory and experiment. A slight phase shift between slices is observed in our experimental data, whereas the fitted model only included a constant phase.

The current magnitude obtained fitting the experimental data (Fig.2) differs from the simulated one by a factor of about 2. This may be due to the limited dynamic range of B_1 values determined using the dual-TR method.

Qualitatively, the current profile observed along the z-axis shows similar behavior, even though the capacitive currents across the isolating varnish seems stronger in the experiment. This is likely due to the difficulty to correctly model the thin isolating film numerically.

Conclusion and perspectives:

This preliminary work paves the way for evaluating the RF safety of long conductive wire using B_1 measurements. The experimental B_1 maps concord well with the theoretical model and the fitted current profile reproduces the behavior observed in EM simulations. Next steps will be to improve the simulation of the thin wire insulation and experimental B_1 maps. The model can be extended in a straightforward way to wires at arbitrary angles with respect to the magnetic field. Finally, given a known wire tip geometry, induced current can be linked to expected SAR and temperature increase.

References and acknowledgment:

[1] Van den Bosch et al.,Med. Phys. 37(2):814-821 (2010). [2] Hoult, Concepts M.R 12:173-187 (2000). [3] ASTM, F2182-09. [4] Yarnykh et al.,MRM 57:192-200 (2007). [5] Leifer et al. MRM 38:726-732 (1997). This work is supported by a grant from the Rhône-Alpes Region.